Development of a method for estimating tank internal conditions during cryogenic fluid filling

Shin Sakai[1*], Takehiro Himeno[1], Tomohito Enoki[2], Motoyuki Kimata[2], Hirokazu Otsubo[2]

[1] The University of Tokyo, Tokyo, Japan
[2]TOYOTA MOTOR CORPORATION, Aichi, Japan

[*]E-mail: sakai@aero.t.u-tokyo.ac.jp

Abstract. A reduced-order model is presented for simulating cryogenic tank filling under thermodynamic non-equilibrium. The tank is represented by a Lagrangian multilayer scheme with variable-size layers; interface relocation and repartitioning enable robust gas–liquid interface tracking without phase-specific branching. A unified control-volume formulation solves single- and two-phase regimes with the same mass and energy balances, simplifying implementation. Pipe–tank coupling incorporates time-resolved cryocooler heat absorption as a direct input, reproducing the sharp initial pressure rise seen in tests. Under static conditions, thermal diffusion through the solid wall dominates internal temperature equalization. The model is validated with liquid-oxygen experiments. The approach provides a practical, computationally efficient tool for cryogenic tank design in space applications; future work will add fluid mixing and extend geometric generality.

1. Research background and aim of this research

As human activity extends to the Moon and Mars, reliable management of cryogenic propellants is critical for long-duration missions. Storage and tank-to-tank transfer must operate under reduced gravity, where fluid behaviour differs from Earth. Precise tank-pressure control requires understanding both fluid dynamics and thermal phenomena. Yet demonstrating reliability during design is difficult and costly; predictive tools that simulate coupled thermal–fluid behaviour over mission timescales are therefore essential.

Recent work spans experiments, modeling, and operations across terrestrial and micro-g settings [1-4]. In general, reduced-order tools for cryogenic tanks typically trade spatial fidelity for speed. NASA's CryoFILL Thermal Desktop model[1], for example, resolves detailed hardware couplings (BAC lines, cryocooler, radiation) but represents the tank interior with one vapor node and one liquid node. No thermal stratification is modelled inside the tank. This is appropriate for hardware-level studies but limits pressure prediction when vertical temperature gradients matter. In contrast, TankSIM[3] is a lumped, multinode transient code that captures self-pressurization, boil-off and pressure-control logic over mission timelines; its nodes comprise ullage, bulk liquid, wall segments, interface, films and droplets, and it has been validated against MHTB hydrogen tests. However, TankSIM still treats each region in a lumped manner rather than resolving vertical stratification with moving interfaces during fills. For on-orbit transfer, fast four-node thermodynamic models have been proposed for no-vent LH_2 filling [4]. These assume a

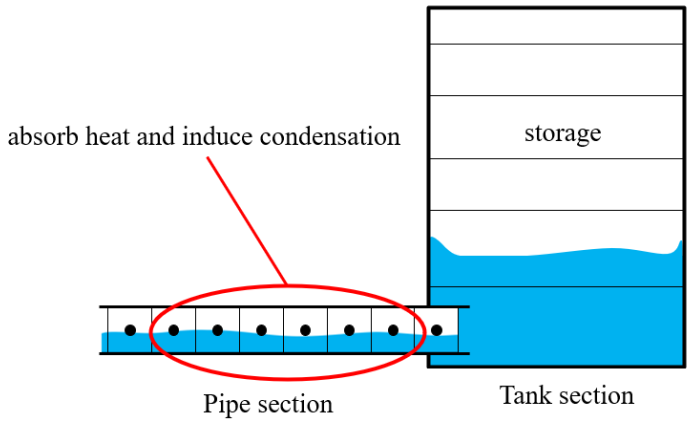

Figure 1. Overview of the system

characteristic phase layout and include micro-gravity-corrected boiling correlations, achieving ≈6% pressure error versus CFD. Yet, by construction, they remain few-node and do not track evolving stratification fields. Collectively, the literature shows a gap for low-dimensional models that (i) resolve stratification/non-equilibrium with moving interfaces, (ii) couple robustly to conductive tank walls, and (iii) remain fast enough for design and control studies.

We address this gap with a layer-wise, Lagrangian tank model that discretizes the fluid column into variable-thickness control volumes and keeps the gas–liquid interface confined to a single moving layer via relocation/repartitioning, so single- and two-phase regimes are advanced by the same mass/energy balances without phase-specific branching. Wall–fluid coupling is treated explicitly (diffusion in the solid plus natural-convection correlations on the fluid side), enabling ablation studies that quantify the wall's role in pressure evolution, while inter-layer exchange is conduction-only to preserve reduced-order tractability (later extended as needed). Compared with prior lumped or few-node approaches, this yields a computationally light, non-equilibrium model that captures stratification and interface motion.

2. Tank filling simulation models

2.1 Overview of the model

We develop a reduced-order model of cryogenic-fluid filling that is suitable for long-duration transients (hours–days) and avoids the cost of full CFD. The system (Fig. 1) comprises a pipeline that cools and delivers the working fluid and a storage tank. Component-level models are formulated and then coupled to obtain the system response.

2.2 Pipe section

Flow in the line is treated as one-dimensional homogeneous two-phase flow. The mass, momentum, and energy equations (1)–(3) are solved numerically with wall friction and condensation. A semi-implicit discretization advances pressure and velocity stably[7][8][9]. The pipe model supplies the tank boundary conditions—mass flow rate and inlet enthalpy—at each system time step.

$$\frac{\partial \rho_m}{\partial t} + \frac{\partial \rho_m u}{\partial z} = 0 \tag{1}$$

$$\frac{\partial u}{\partial t} + u\frac{\partial u}{\partial z} = -\frac{1}{\rho_m}\frac{\partial P}{\partial z} - \frac{F_w}{\rho_m} \tag{2}$$

$$\frac{\partial \rho_m h}{\partial t} + \frac{\partial \rho_m u h}{\partial z} = \frac{\partial P}{\partial t} + u\frac{\partial P}{\partial z} + q \tag{3}$$

2.3 Tank section

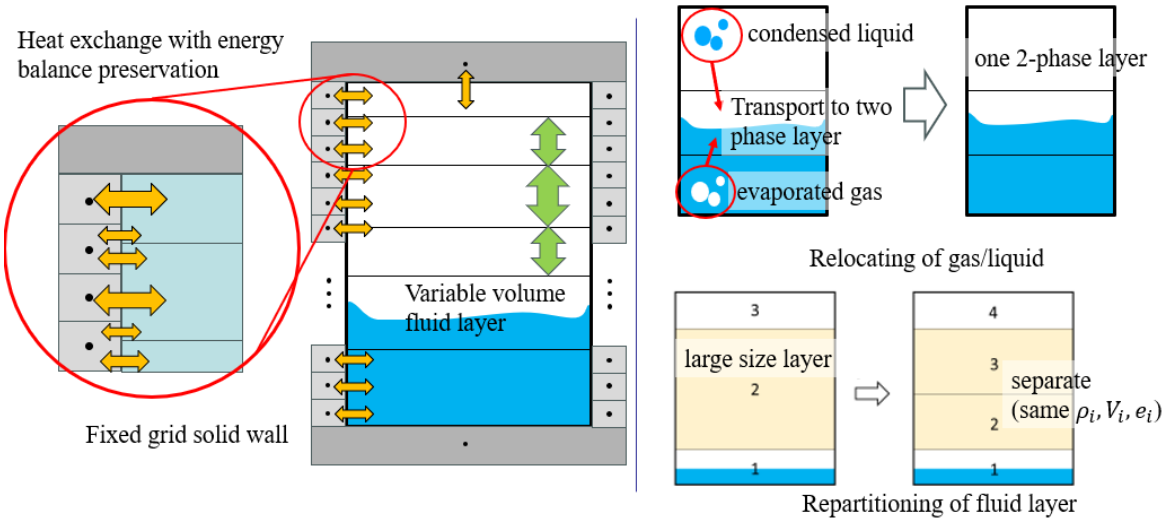

Figure 2. Detail of tank model

The tank is discretized vertically into Lagrangian layers of variable thickness. Each layer is a control volume in thermal equilibrium (gas, liquid, or saturated two-phase), advanced by mass- and energy-balance equations (4)–(5) under spatially uniform pressure. No momentum equation is solved in the tank; "Lagrangian" denotes vertical motion of layer boundaries for interface tracking, not intralayer advection. Momentum is solved only in the 1-D pipe model (Sec. 2.2).

$$\frac{\partial}{\partial t}(\rho_i V_i) = \dot{m}_i \tag{4}$$

$$\frac{\partial}{\partial t}(\rho_i V_i e_i) + p\frac{\partial V_i}{\partial t} = \dot{m}_i h_{in} + q_i \tag{5}$$

Vertical heat exchange between layers is modeled solely by conduction; bulk advection/mixing, sloshing, and bubble-induced mixing are not resolved. This deliberate simplification increases thermal stratification relative to reality—especially during Phase 2—and can bias pressure, as discussed in Secs. 4.1 and 4.3.

The tank wall is represented by a fixed Eulerian mesh (Fig. 2, left) and solves transient heat conduction. Heat transfer on the fluid side uses Churchill's correlation[6] for natural convection around a vertical plate, with the usual definitions of Ra with layer height x and Pr (Eq. 6). Wall–fluid heat fluxes enter the layer energy balances.

$$\mathrm{Nu} = \left(0.825 + \frac{0.387\mathrm{Ra}^{1/6}}{\left(1 + \left(\frac{0.492}{\mathrm{Pr}}\right)^{9/16}\right)^{8/27}} \right)^2 \tag{6}$$

$$\mathrm{Ra} = \frac{g\beta(T_w - T_f)x^3}{\nu\alpha}, \mathrm{Pr} = \frac{\nu}{\alpha}$$

For the fluid layers, two numerical techniques are implemented to enhance model stability and resolution (see Fig. 2 right). Mass produced by phase change is relocated to the interface layer each step so that the interface remains confined to a single layer; layers whose volume exceeds a threshold are repartitioned to maintain vertical resolution. This mechanism maintains vertical spatial resolution throughout the simulation by dynamically redistributing mass and energy across layers.

To keep the gas–liquid interface confined to a single layer and to preserve resolution (Fig. 2, right), two algorithmic devices are used each time step, after layer update according to eq. (4)(5): (i) Relocation. Mass produced by phase change is transported to the unique interface layer at constant pressure; transported mass/energy (Δm, ΔE) are accumulated there to maintain exact conservation. (ii) Repartitioning**.** Layers whose volume exceeds a threshold are bisected conservatively. For a two-phase layer, the split is biased so that liquid remains below the interface. These steps are purely numerical; no additional interfacial heat-transfer law is introduced beyond conduction between adjacent layers and wall coupling.

We neglect bulk advection within layers and model vertical heat exchange solely by conduction. This assumption is based on the current static conditions and the fact that the solid wall provides the dominant thermal path for equalisation in the situation dealing with here. Consistently, numerical experiments with and without wall diffusion (Patterns A–C) indicate that wall-coupled diffusion governs the spread of temperature and the pressure evolution (sec. 4.3). The treatment of heat transfer between layers as thermal conduction only can be evaluated by making a comparison with the case of complete mixing inside the tank. This appears as an underestimation of the tank internal pressure in the initial stage of filling (sec. 4.1).

3. Experiments on ground with liquid Oxygen

3.1 Setups and conditions

The proposed model was validated against experimental results obtained from ground-based tests using liquid oxygen. An overview of the experimental setup is shown in Fig. 3. Gaseous

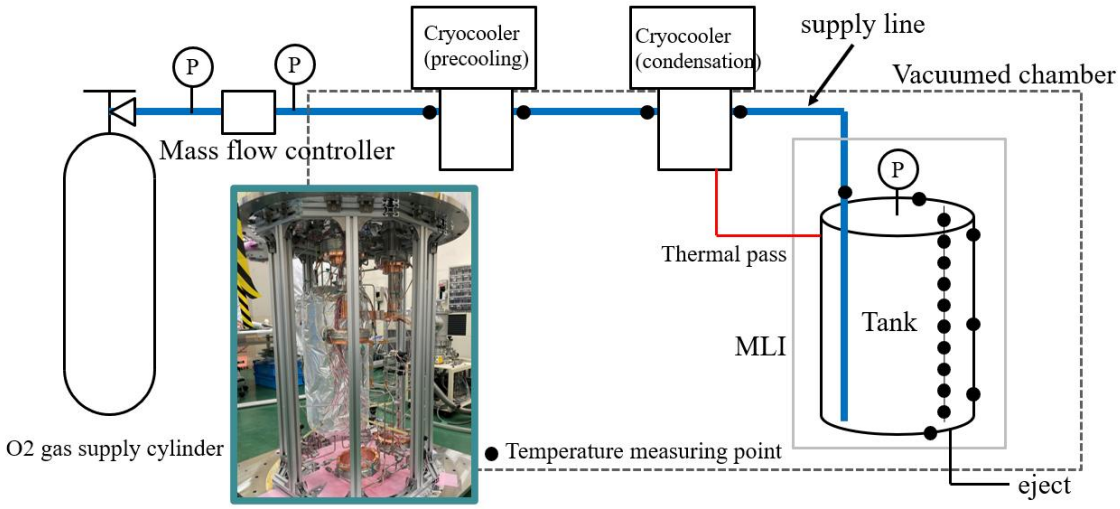

Figure 3. Overview of experimental setup. The equipment was produced by Sumitomo Heavy Industries (SHI).

Table 1. Experimental conditions

	Liquid filling	Liquid measure	Tank init. Temp.	Tank init. Press.	Cryocooler output
LOX#3	Continuous	0→90 %	140.5 K	1.0 MPa	Frequently ON
LOX#5	Continuous	0→90 %	135.5 K	1.0 MPa	Frequently ON

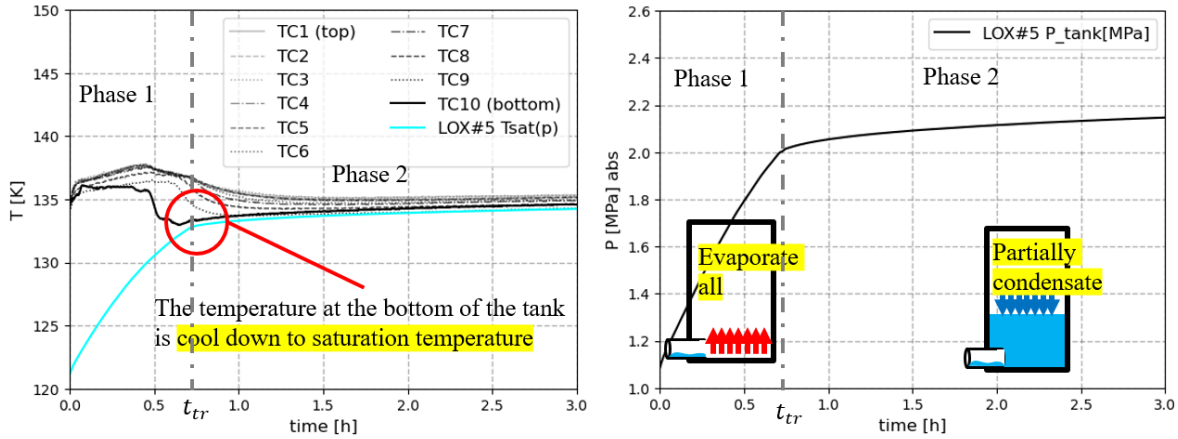

(a) Tank internal temperature (b) Tank internal pressure

Figure 4. (a) Tank internal temperatures measured by ten evenly spaced thermocouples (TC1–TC10 from top to bottom) and saturation temperature $T_{sat}(P)$ computed from the measured tank pressure. (b) Absolute tank pressure p_{tank}. The vertical line marks the onset of liquid accumulation t_{tr}, which separates Phase 1 (no sustained liquid inventory) and Phase 2 (with liquid pool).

oxygen was supplied from an upstream cylinder, with the flow rate regulated by a mass flow controller. The gas was subsequently cooled and condensed through a two-stage chilling system comprising a pre-cooler and a condenser, resulting in subcooled liquid oxygen. This subcooled liquid was then introduced into the storage tank. The entire experiment was conducted within a vacuum chamber, and the tank was further thermally insulated using multilayer insulation (MLI) to minimize external heat ingress.

The experimental conditions are summarized in Table 1. Filling tests were conducted under two different initial temperature conditions to evaluate the influence of thermal state on the filling behavior.

3.2 Summary of filling experimental results

Fig. 4 summarizes the LOX#5 fill. Fig. 4(a) shows ten thermocouples TC1–TC10 (top→bottom); the cyan curve is the saturation temperature $T_{sat}(p)$ calculated from the measured tank pressure using oxygen properties (REFPROP). Fig. 4(b) shows the absolute internal tank pressure p_{tank}. We distinguish two regimes by a quantitative criterion. Phase 1 (no sustained liquid inventory) holds while $\min T_i(t) > T_{sat}(p)$. All injected liquid evaporates and pressure rises rapidly (in fact, there is an effect of insufficient cooling of the injected liquid due to the initial lag of heat absorption).The transition time t_{tr} is defined as the first instant when $\min T_i(t) < T_{sat}(p)$. Phase 2 begins thereafter, with liquid pooling at the bottom and partial condensation in the ullage; correspondingly, the pressure slope decreases. LOX#3 exhibits the same behaviour.

4. Model validation

4.1 Analysis of important factors of pressure history by numerical experiment

We evaluate which inputs predominantly shape the absolute tank pressure: (i) the initial thermal state (wall/ullage temperatures), (ii) the time-resolved cryocooler heat absorption, and (iii) the degree of thermal non-equilibrium (layered vs well-mixed). Throughout Fig. 5, the vertical dashed line marks the Phase 1→2 transition time t_{tr} (see sec.3.2). Experimentally, t_{tr} is when the lowest thermocouple first meets $T_{sat}(p)$; in the model, when the bottom layer's liquid fraction exceeds zero. In (i), raising the initial wall temperature increases p_{tank} and shifts t_{tr} later, consistent with the wall's larger heat capacity. In (ii), using the measured $\dot{Q}_{cool}(t)$ (equal total heat to the

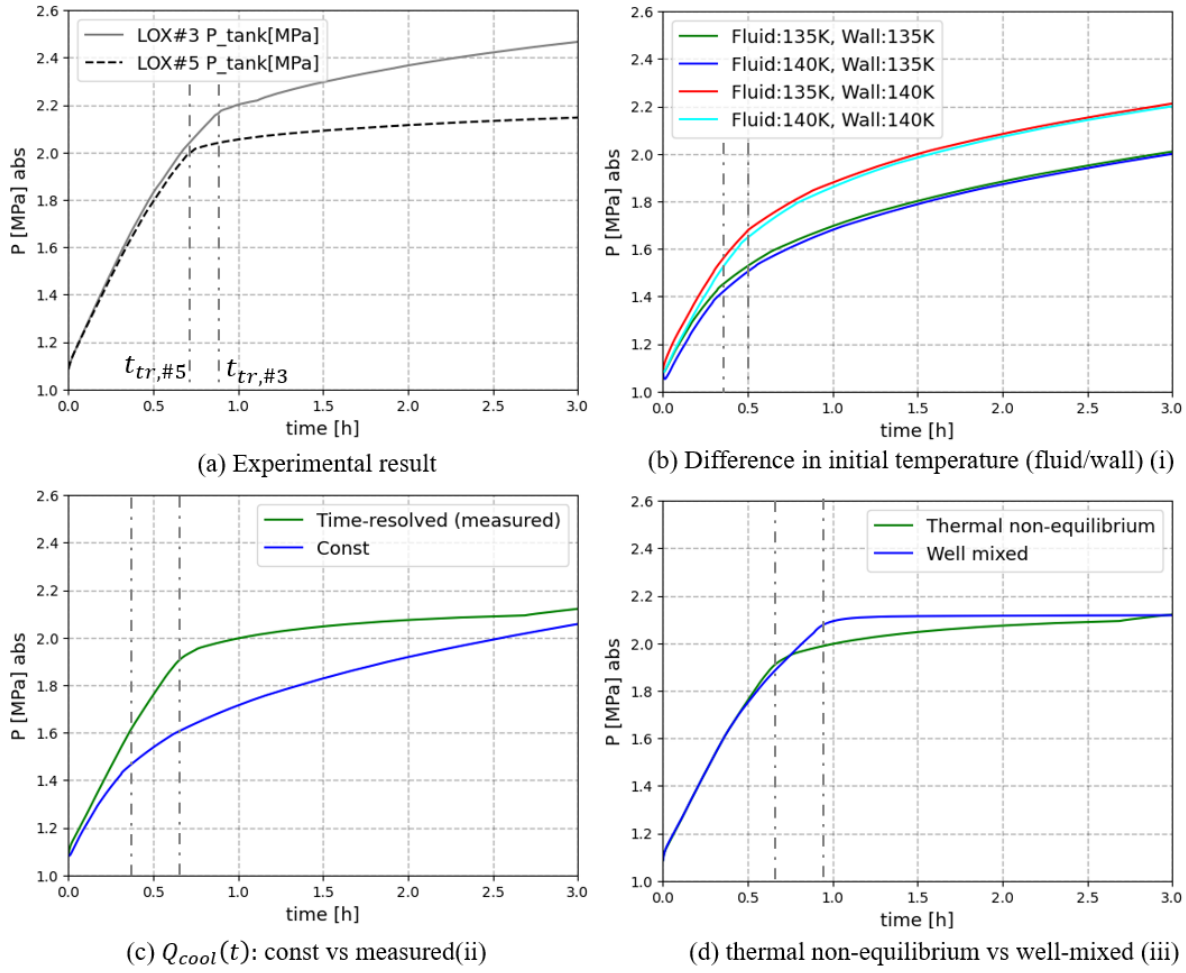

(a) Experimental result

(b) Difference in initial temperature (fluid/wall) (i)

(c) $Q_{cool}(t)$: const vs measured(ii)

(d) thermal non-equilibrium vs well-mixed (iii)

Figure 5. Important factors for tank internal pressure

constant-rate case) reproduces the sharp early rise observed in tests, capturing the initial under-cooled inflow. In (iii), the layered non-equilibrium model transitions earlier and continue to rise gradually p_{tank} in Phase 2 than the well-mixed model; as stratification relaxes, the predictions converge.

4.2 Comparision with experimental results

The results of the numerical simulations were compared with the experimental data. Fig. 6 presents the comparison between the test and simulation results. Figure 6(a), (c) shows the pressure histories under the two test conditions, while Figures 6(b), (d) illustrate the corresponding temperature distribution histories. Overall, the model demonstrates good agreement with the measured pressure histories. However, the predicted temperature distributions exhibit a broader spatial extent than those observed in the experiments. This discrepancy is likely attributable to the omission of thermal effects associated with tank outfitting and ancillary components in the current model. A more detailed discussion of these factors is provided in the following section.

4.3 Effect of tank solid wall: ablation study (model-only)

To explain the discrepancy noted in Sec. 4.2 (Fig. 6), we conduct a model-only ablation of wall coupling and diffusion. Experimental comparisons are provided in Sec. 4.2. Figure 7 isolates wall-related mechanisms via a model-only ablation: A (no fluid–wall heat transfer), B (wall coupling without wall diffusion), and C (full coupling with realistic wall diffusion). In panels (b)–(c), bold

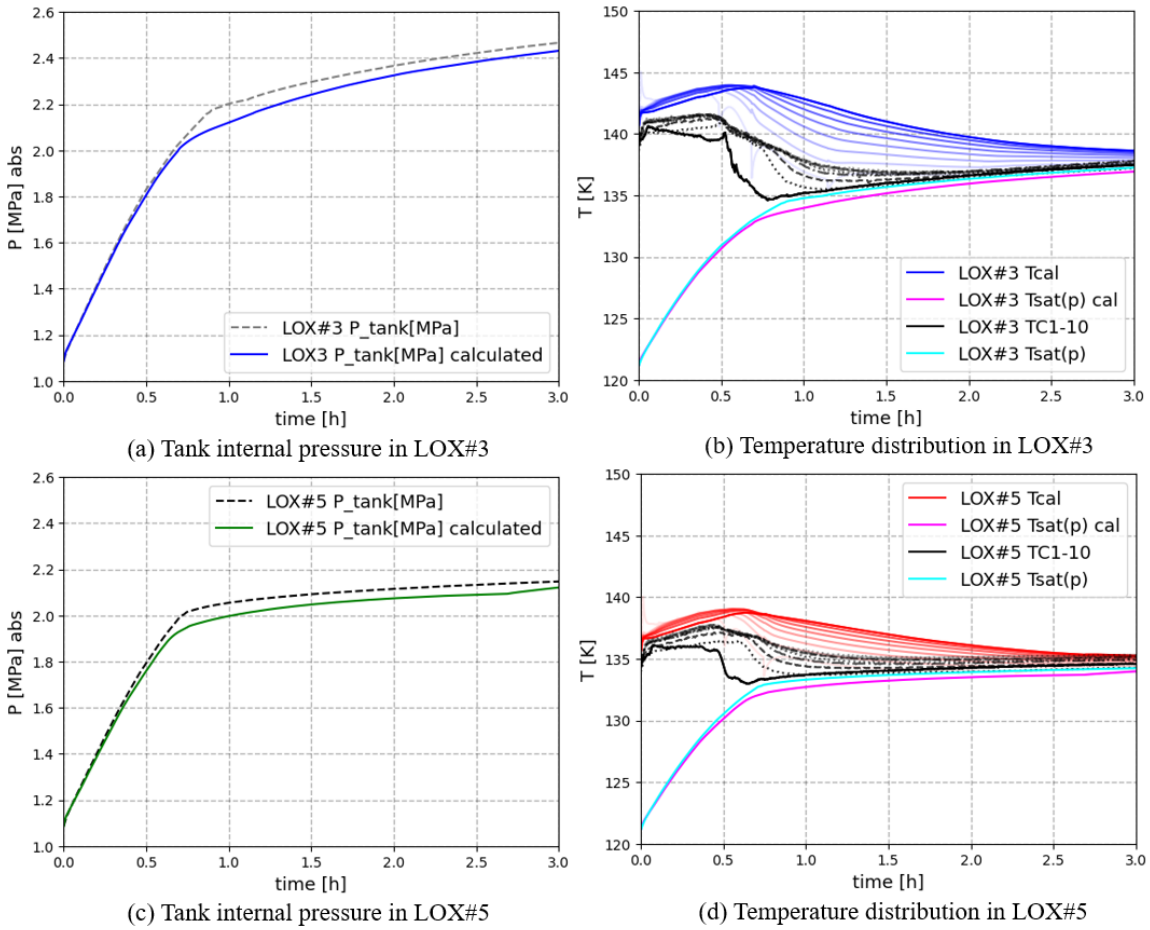

(a) Tank internal pressure in LOX#3 (b) Temperature distribution in LOX#3

(c) Tank internal pressure in LOX#5 (d) Temperature distribution in LOX#5

Figure 6. Comparison between model predictions and experimental results. (Blue and red lines in (b) and (d) are calculated temperature values at the same position of the thermometer in the experiment)

solid and bold dashed curves denote top and bottom layers, respectively; thin faint curves show intermediate layers. Relative to A, B suppresses the early gas-phase overheating above the liquid due to the wall acting as a heat sink, adding wall diffusion (C) further spreads heat vertically, acting as a lateral thermal path through the structure. This moves the model toward the narrower stratification seen in the measurements (see Sec. 4.2, Fig. 5), although full agreement is not reached—consistent with unmodelled thermal paths (e.g., penetrations, vertical piping).

5. Conclusion

We presented a reduced-order model for cryogenic tank filling that captures thermodynamic non-equilibrium via a Lagrangian, variable-layer formulation with interface relocation/repartitioning and a coupled pipe–tank treatment. Driven by time-resolved cryocooler heat absorption, the model reproduces the two-stage pressure evolution and sharp initial rise observed in LOX ground tests. Sensitivity studies identify initial wall temperature, the temporal profile of heat removal, and thermal stratification as the dominant controls; wall-mediated diffusion emerges as the primary path for temperature equalization. Remaining discrepancies in temperature fields are attributable to unmodeled thermal pathways in hardware, while pressure predictions remain robust. The current scope neglects bulk mixing and gravity-dependent wall boiling/condensation and uses conduction-only inter-layer exchange, with validity demonstrated for vertical cylindrical tanks. Future work will incorporate validated, gravity-sensitive boiling/condensation and mixing models and extend applicability across geometries and

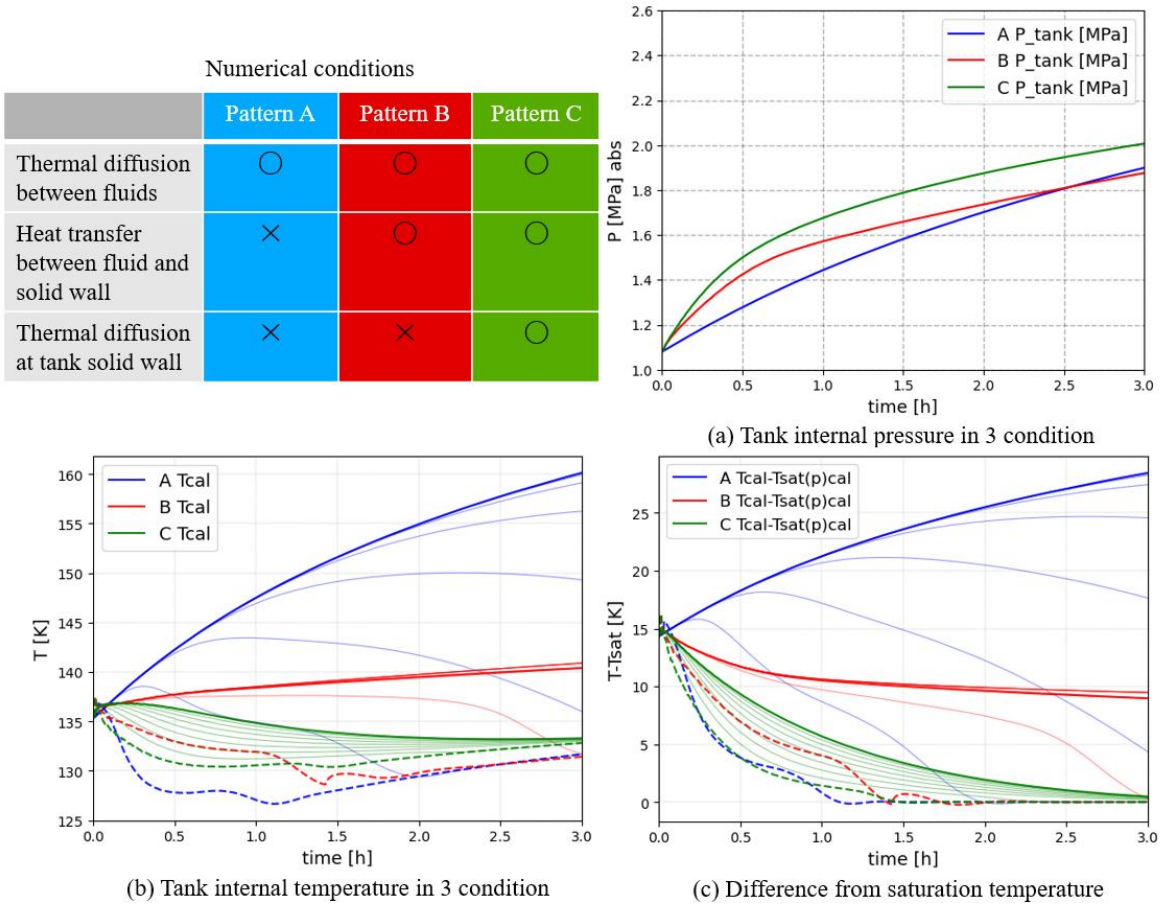

Figure 7. Comparison of numerical ablation results: Pattern A, B, and C (In (b)–(c), bold solid and bold dashed curves denote top and bottom layers, respectively; thin faint curves show intermediate layers.)

reduced-gravity conditions. A minimal parametric wall phase-change coefficient scaling with g (e.g., proportional to |Tsat−Tw| with a gravity-dependent factor) will be trialled to bound gravity sensitivity before adopting validated pool-boiling correlations in low-g.

References

[1] Kashani, A., et al. "Thermal Modeling of CryoFILL liquefaction tests." IOP Conference Series: Materials Science and Engineering. Vol. 1301. No. 1. IOP Publishing, 2024.
[2] Jones, J. R., and James E. Fesmire. "Quick cooling and filling through a single port for cryogenic transfer operations." AIP Conference Proceedings. Vol. 613. No. 1. American Institute of Physics, 2002.
[3] Bolshinskiy, L. G., et al. “Tank system integrated model: a cryogenic tank performance prediction program.” No. M-1431. 2017.
[4] Ma, Yuan, et al. "Analysis and modeling of no-vent filling process for liquid-hydrogen tank in orbital conditions." Processes 11.5 (2023): 1315.
[5] E. W. Lemmon, I. H. Bell, M. L. Huber, and M. O. McLinden, NIST Standard Reference Database 23: “Reference Fluid Thermodynamic and Transport Properties (REFPROP)”, Version 10.0, National Institute of Standards and Technology, Gaithersburg, 2018.
[6] Churchill, Stuart W., and Humbert HS Chu. "Correlating equations for laminar and turbulent free convection from a vertical plate." *International journal of heat and mass transfer* 18.11 (1975): 1323-1329.
[7] Breber, G., J. W. Palen, and J. Taborek. ”Prediction of horizontal tubeside condensation of pure components using flow regime criteria.” (1980): 471-476.
[8] The Japan Society of Mechanical Engineers (JSME), Ed., “Handbook of gas-liquid two-phase flow technology”, Corona Publishing Co., Ltd., 1989 (in Japanese).
[9] The Atomic Energy Society of Japan (AESJ), Ed., “Numerical Analysis of Gas-Liquid Two-Phase Flow”. Asakura Publishing Co., Ltd., 1993 (in Japanese).